A Comparison of Alumina, Carbon, and Carbon-Covered Alumina as Supports for Ni–Mo–F Additives: Carbon Deposition and Model Compound Reaction Studies

P. M. BOORMAN, K. CHONG, R. A. KYDD,[1] and J. M. Lewis

Department of Chemistry, University of Calgary, Calgary, Alberta, Canada T2N 1N4

Fluoride-promoted Ni–Mo catalysts supported on alumina, carbon, and carbon-covered alumina have been investigated for their activity in cumene cracking, hydrocracking (reduced and sulfided forms), and thiophene HDS. The carbon-covered alumina was prepared by pyrolysis of cyclohexene over either γ-alumina or boehmite and the carbon deposition followed adsorption isotherm-type behavior. The cumene reaction studies indicate that the resulting support system successfully merges the properties of carbon and alumina, possessing improved dehydrogenation–hydrogenation functionality due to carbon and acidic properties due to alumina, such as the generation of Brønsted acidity upon fluoride impregnation. In the thiophene HDS reaction the catalyst activities followed the order $Al_2O_3 > C–Al_2O_3 > C$, suggesting that alumina, and not carbon, is the superior HDS support at atmospheric H_2 pressure and at the metal loadings used in this study. Carbon deposition onto Ni–Mo–F/Al_2O_3 catalysts revealed that cyclohexene polymerization is promoted by the metal centers, resulting in multilayer islands on these sites, and not by the fluoride-associated Brønsted acid sites. However, the Brønsted acid sites do promote coke formation when the polymerization reaction is easier, such as for α-methylstyrene. © 1991 Academic Press, Inc.

INTRODUCTION

Alumina is the most widely used support material for commercial Co- or Ni-promoted molybdenum hydrotreating catalysts. Notable features of alumina supports are their ability to disperse up to 20 wt% of the active metal phase (*1*) and good mechanical properties. However, a considerable drawback with alumina is the unwanted strong metal–support interactions, especially at low loadings, which may impede desirable reactions, e.g., conversion of the metal oxides into the active sulfide phase (*2*). Furthermore, the promoter metals can interact with the alumina to form $CoAl_2O_4$ or $NiAl_2O_4$ or they can occupy octahedral or tetrahedral sites inside the alumina lattice, both of which render them catalytically inactive (*3, 4*). The quest for superior support systems has led researchers to explore alternative support materials.

One such support system which has received attention is carbon. This is due to the many attributes linked with carbon such as high surface areas with a controlled pore volume, reduced coking propensity (*5*), resistance to nitrogen poisoning (*6*), easy metals recovery by burning off the support, and variable surface functional groups, all giving carbon tremendous scope as a support material. For these reasons, Vissers *et al.* and other researchers have been investigating carbon-supported metal sulfides in recent years (*7–11*). Superior thiophene hydrodesulfurization activity for carbon-supported catalysts over their silica and alumina counterparts, due to a weaker metal–support interaction for carbon ascribed to the inertness of carbon, has been reported. However, aside from these attributes, disadvantages can also be discerned. While activated carbons do possess high surface area, much of this area may be in meso- and micropores (radius <25 nm). Due to diffusion limitations, this may seriously

[1] To whom correspondence should be addressed.

limit the utility of active phases deposited in these pores. Also, although the carbon surface offers a variety of oxygen functionalities, the nature of activated carbon is amorphous. Thus the nature and concentration of these groups may be insufficient for high dispersion and inadequate to facilitate certain reactions. Another drawback, particularly for an industrial application, may be the poor mechanical properties of carbons.

Clearly, both alumina and carbon have advantages and disadvantages as supports. An ideal support may result by merging the attributes of both support systems. If the alumina surface is coated with a thin layer of carbon, the resulting support may inherit the favorable physical properties of alumina while also retaining the reduced coking propensity and hydrogenation activity associated with carbon. The alumina surface can be coated with carbon by the pyrolysis of organic precursors (12–14). Sulfided Co catalysts supported on carbon-covered alumina were investigated by Vissers et al. (14). The activities of these catalysts for thiophene hydrodesulfurization were intermediate between those of carbon and alumina supports. The carbon coverage was nonuniform and the activity increased with increasing carbon content of the support, a testimony to the reduced metal–support interaction.

Much of the research into catalyst development for hydroprocessing has focused on sulfided metal catalysts for heteroatom removal, in particular sulfur. However, a practical hydroprocessing catalyst for real feedstocks must be capable not only of sulfur removal but also of hydrogenating and hydrocracking high-molecular-weight components of the feed. Previous work in our laboratory using cumene as a model compound and Co–Mo/Al$_2$O$_3$ and Ni–Mo/Al$_2$O$_3$ catalysts has shown that fluoride addition enhances the cracking activity (15–17). The fluoride is thought to replace some surface hydroxide (and oxide?) groups, thereby po-

larizing the alumina lattice and increasing the acidity of the remaining hydroxyls. The Brønsted acid sites created in this way facilitate carbocation reactions such as cumene dealkylation to benzene. Our results, in conjunction with the improved hydrodesulfurization activity reported for Co/carbon-covered alumina- compared to alumina-supported catalysts (14), have prompted us to extend our study of fluoride promotion to this support as well.

The aim of the present work is to explore the role of support and fluoride promotion in hydrotreating and hydrocracking applications. Thus a series of fluoride-promoted Ni–Mo catalysts supported on carbon-covered alumina have been investigated for their activity, selectivity, and deactivation characteristics for cumene cracking (oxides), cumene hydrocracking (reduced and sulfided), and thiophene hydrodesulfurization. A comparison to analogous catalysts supported on carbon and alumina has also been undertaken, and carbon coating of the alumina catalysts investigated. It was envisaged that the better hydrogenation capability and possibly reduced coking propensity (deactivation) for carbon in concert with the enhanced cracking ability for fluorided alumina may make fluorided Ni–Mo supported on carbon-covered alumina an attractive hydroprocessing catalyst.

EXPERIMENTAL

Catalyst Preparation

The catalysts were prepared by dry impregnation of the supports, γ-alumina, carbon, and carbon-covered alumina, with the additives dissolved in a minimum volume of distilled water onto the support materials to give 3 wt% NiO, 15 wt% MoO$_3$, and various nominal fluoride concentrations. (NH$_4$)$_6$Mo$_7$O$_{24}$4H$_2$O, Ni(NO$_3$)$_2$6H$_2$O, and NH$_4$F were used as the source of Mo, Ni, and fluoride, respectively. The order of addition was Mo, followed by Ni, followed by fluoride, with no drying steps in between. If one or more additives were absent, pure

water was added so that the amount of water used was the same in each case. The catalyst was mulled for 1–2 min after each addition and was not subjected to a calcination between additions. The catalyst was left to dry in air at room temperature overnight followed by drying at 100°C overnight. At this stage, the alumina-supported catalysts were calcined by heating at 4°C/min to 500°C and maintaining this temperature for 4 hr under a stream of air. The carbon and carbon-covered alumina catalysts were not calcined because oxidative degradation would occur.

The preparation of the γ-alumina support has been described previously (17). The activated carbon used in this study was Darco KB from the Aldrich Chemical Company. It was used as supplied following drying at 100°C for 24 hr. The carbon-coated alumina was prepared as by Vissers et al. (14) by pyrolyzing cyclohexene at 600°C. Approximately 2 g of γ-alumina was placed in a calcination tube and heated to 600°C at a rate of 10°C/min under a dry N_2 flow of 20 ml/min. It was held at 600°C for $\frac{1}{2}$ hr, after which the N_2 was bubbled through cyclohexene, held at room temperature, before passing over the alumina for 6 hr at 600°C. The sample was allowed to cool under a flow of dry N_2. The same procedure was applied to the catalysts supported on alumina for the AC series of catalysts (see Table 1). These catalysts were carbon-coated after the additives had been impregnated. Table 1 gives the designations assigned to the various catalysts.

Catalyst Testing and Characterization

As described previously (17), the catalyst testing was carried out in a stainless steel, continuous flow, fixed bed bench top reactor equipped with an on-line gas chromatograph. The reactor (15 mm i.d.) was packed with 0.15 g of 80–100 mesh catalyst between layers of quartz wool and the model compound, cumene or thiophene, was held in a presaturator at 15 ± 1°C upstream from the reactor. Catalyst activation was achieved at 500°C under either He (for cumene cracking), H_2 (for the reduced catalysts in hydrocracking), or 10% H_2S/H_2 (for the sulfided catalysts in HDS or hydrocracking reactions). The reactant model compound was carried over the catalyst by bubbling the appropriate sweep gas through the presaturator, i.e., He for cumene cracking and H_2 for hydrocracking and HDS reactions. The products were analyzed every 10 (HDS) or 20 min by on-line gas chromatography and percent conversions calculated. The reaction was stopped after 4 h, at which time the % conversion had reached an approximately constant value.

Alumina catalysts (A series), carbon-covered alumina catalysts (CA series), and alumina catalysts carbon covered (AC series) were prepared for fluoride analysis using a similar procedure to that described by Swift and Schaefer (18). This involved fusing 50 mg of the sample with 0.5 g of Na_2CO_3, 0.25 g $NaNO_3$, and 0.5 g $NaOH$ in a nickel crucible. After being cooled, this mixture was dissolved in 5 ml distilled water and 95 ml of TISAB IV (Orion Research) was added as a buffer and Al^{3+} complexing agent. 50 mg of γ-Al_2O_3 fused as above was dissolved in 5 ml of fluoride solution of varying concentration to prepare the standards. Fluoride analysis was then carried out with a fluoride sensitive electrode. For the carbon catalysts, stirring of ~0.1 g catalyst in 10 ml 0.1 M NaOH overnight was sufficient to dissolve the fluoride present. The catalysts were filtered and the solution analyzed for fluoride as above.

The surface areas of the catalysts before activation were measured by the BET method, with N_2 as the absorbent, using a Micromeritics high-speed surface area analyzer. The pore size distribution data for some of the catalysts was determined by mercury porosimetry using a Quantachrome Autoscan 60. The carbon analyses were performed using a Perkin Elmer 240B CHN Elemental Analyzer. The measured surface

TABLE 1

Composition and Surface Areas of Catalysts

Support	Catalyst	Wt.% additives				Wt.% carbon	Surface area (m²/g)
		NiO	MoO$_3$	F$_{nom.}^{a}$	F$_{meas.}^{a}$		
γ-Al$_2$O$_3$	A1	0	0	0	—	↑	190
	A2	3	15	0	—	NA	137
	A3	3	15	1.8	1.8		125
	A4	3	15	3.6	3.5		122
	A5	3	15	6.9	6.4		113
	A6	0	0	3.6	3.7		186
	A7	0	0	6.9	6.5	↓	177
Carbon	C1	0	0	0	—	↑	1342
	C2	3	15	0	—	NA	891
	C3	3	15	1.8	0.5		802
	C4	3	15	3.6	1.2		810
	C5	3	15	6.9	2.2		827
	C6	0	0	3.6	0.5		1226
	C7	0	0	6.9	0.8	↓	1193
C/Al$_2$O$_3$	CA1	0	0	0	—	↑	144
	CA2	3	15	0	—	9	121
	CA3	3	15	1.8	1.3		92
	CA4	3	15	3.6	2.5		107
	CA5	3	15	6.9	5.4		78
	CA6	0	0	3.6	3.3		147
	CA7	0	0	6.9	6.4	↓	140
C-covered A series	AC2	3	15	0	—	20	130
	AC3	3	15	1.8	1.7	20	105
	AC4	3	15	3.6	3.7	19	106
	AC5	3	15	6.9	5.4	30	108
	AC6	0	0	3.6	3.1	10	128
	AC7	0	0	6.9	4.4	10	116

[a] For A and AC catalysts quoted wt% F are calculated based on the weight of the alumina support. For CA catalysts quoted wt% F are based on the weight of the C/Al$_2$O$_3$ support.

areas and carbon analyses are given in Table 1.

RESULTS AND DISCUSSION

Properties of C-Covered Alumina

The preparation procedure of carbon-covered alumina followed that used by Vissers et al. (14) involving the pyrolysis of cyclohexene over alumina at 600°C for 6 h. While comparable carbon coverage of the alumina was obtained, a decrease, rather than the previously observed increase (14), in the surface area of the resulting support

was observed (from 190 m²g^{-1} for γ-alumina to 144 m²g^{-1} for C–Al$_2$O$_3$). In an attempt to understand this difference, other carbon-covered alumina samples were prepared by varying the pyrolysis time (6 to 48 hr) and by using boehmite or γ-alumina as the precursor support. While increasing weight percent carbon was observed with increasing pyrolysis time, we were unable to increase the surface area of the precursor support. In fact, a linear decrease in surface area was found (Fig. 1). This decrease in surface area is independent of the precursor support, although boehmite appears to pres-
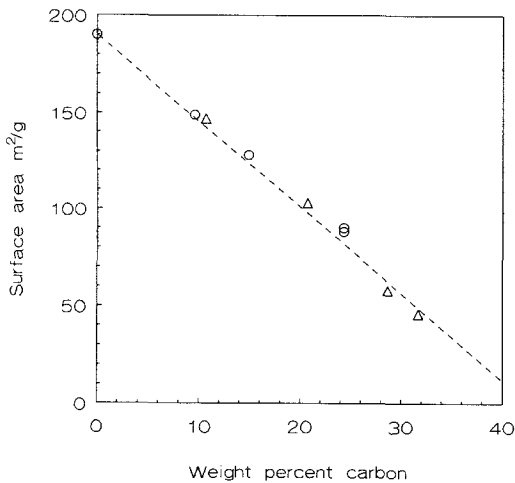
FIG. 1. Effect of C on the surface area of γ-alumina (O) and boehmite (△).

ent the more active cyclohexene pyrolyzing surface, as reflected in a higher weight percent carbon deposited on boehmite compared to γ-alumina for the same pyrolysis time as is demonstrated in Fig. 2. For both γ-alumina and boehmite precursors the curves follow adsorption isotherm type behavior with apparent monolayer carbon coverage
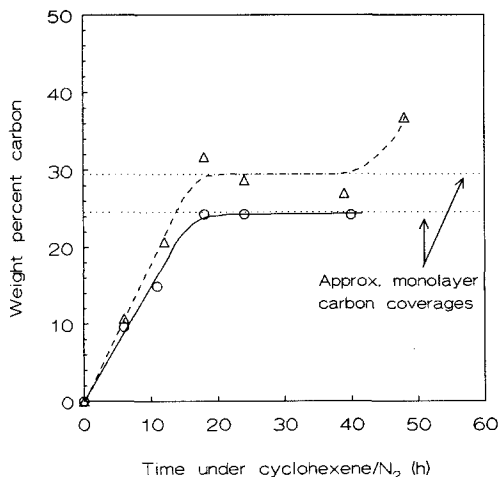

FIG. 2. Effect of cyclohexene pyrolysis time on the weight percent of carbon deposited for γ-alumina (O) and boehmite (△) precursors.

at around 24 and 29 wt% C, respectively. These monolayer carbon coverages imply surface areas of approximately 190 m^2g^{-1} for the γ-alumina and 230 m^2g^{-1} for the transformed boehmite (to γ-alumina) if it is assumed that the deposited carbon possesses a graphite-like structure (12). These surface areas agree well with the values expected for γ-alumina prepared from boehmite and indicate that no appreciable loss in surface area occurs as a result of the high temperature employed in the pyrolysis procedure.

Vissers et al. (14) recognized the possibility of decreasing surface area with carbon coating if the carbon is deposited as a monolayer. Clearly, the conditions required for the deposition of high-surface-area hemispherical carbon particles as discussed by them are very exacting, and despite careful adherence to the procedure described by them we observed only low-surface-area carbon deposition.

In order to investigate whether monolayer carbon coverage of the alumina had indeed been reached, fluoride was impregnated onto one of the carbon-coated alumina samples with 28 wt% C. As discussed later in this paper, fluoride has no affect on the acidity of carbon surfaces and furthermore is not retained by this type of surface, particularly under reaction conditions (19). However, the presence of fluoride has a dramatic effect on the acidity of alumina, resulting in high cracking activity (20) and, furthermore, the loss of fluoride after such a reaction is quite small (17), confirming that the fluoride is bonded to the surface. Therefore both cracking reaction and fluoride analysis before and after this reaction will indicate whether any of the alumina surface remains exposed to fluoride at this loading of carbon.

Sufficient fluoride was contacted with the 28% C–Al_2O_3 to produce a catalyst of 3.6 wt% F and the preparation followed the procedure used for the CA series of catalysts. However, analysis indicated that the actual weight percent fluoride present was 1.1%.

While this is more than that retained by a carbon support, it is less than that retained by an alumina support (cf. C6 and A6 in Table 1) and suggests that some of the alumina surface is still accessible to fluoride. Further evidence that the fluoride was bonded to the alumina surface was provided by the analysis of the spent catalyst after cumene cracking which showed that almost all of the fluoride (1.0%) was still retained. However, the activity of the catalyst in this reaction indicated that the surface possessed no surface acidity; the only product at any time during the reaction was α-methylstyrene, which presumably forms over the deposited carbon, and a yield of 8.3% is comparable to that seen for CA1 (9% C–Al$_2$O$_3$) i.e., 8.9% as shown in Table 2. The conclusions drawn from this are, therefore, that some of the alumina surface is still accessible to fluoride, possibly the small pores of the C-covered alumina, but the Brønsted sites which develop are inaccessible to cumene and also to cyclohexene; i.e., a monolayer coverage of carbon has been reached with respect to that part of the surface which is accessible to cyclohexene (and cumene).

Catalyst Compositions and Surface Areas

The compositions of the catalysts used in this study are given in Table 1 together with their surface areas, measured weight percent fluoride, and, where applicable, weight percent carbon. Four series of catalysts were investigated: Ni–Mo–F supported on C-coated alumina (CA); Ni–Mo–F/Al$_2$O$_3$ (A) and Ni–Mo–F/C (C) as comparisons; and also C-coated Ni–Mo–F/Al$_2$O$_3$ (AC). All these catalysts had comparable nominal weight percents of the additives, based on the weight of the different supports. The measured wt% F was in good agreement with the nominal wt% for the A series of catalysts and fair agreement for the CA and AC catalysts. The apparent lower F content of these catalysts, especially for the AC series, may be due in part to the uncertainty in the precise weight percent carbon they contain (see later). The measured fluoride content of the carbon catalysts was much lower than expected, a consequence of the inertness of the carbon support toward reaction with F$^-$.

For all catalysts, with the exception of CA6, fluoride produces a small decrease in surface area. Metal additives produce somewhat larger decreases. This has been observed previously by us for alumina-supported fluorided Ni–Mo catalysts (17).

Some interesting observations arise from the results of cyclohexene pyrolysis over the alumina (A) series of catalysts to give the AC series. For those catalysts containing fluoride only, the weight percent of carbon deposited is comparable to that on alumina only (9–10 wt%) and a similar large decrease in surface area is seen after carbon deposition. This implies that fluoride does not promote cyclohexene polymerization. However, model compound reactions indicate that enough carbon is present to poison the fluoride-associated Brønsted acid sites generated by up to 3.6 wt% F$^-$ (see the next section). This suggests that while the fluoride does not promote the polymerization, carbon is nevertheless deposited on these sites. In contrast, for catalysts containing metal additives, substantially more carbon is deposited (19–30 wt%) and only small decreases in surface area result. This implies that either some of the carbon deposited has a high surface area, or carbon deposition does not occur uniformly over the catalyst, but rather, in "islands," apparently on the metal sites. Model compound studies, the results of which are discussed in more detail in later sections, indicate the latter. Furthermore, carbon analysis of the metal-containing AC catalysts revealed that these samples only were inhomogeneous (hence quoted C weight percents are approximate, in the range ±3 wt% C for AC2–4, and ±5 wt% C for AC5). This provides further support for the argument that the carbon is deposited on islands on these catalysts.

One possible explanation of these observations is that, for the A series, both the

TABLE 2

Model Compound Testing Results after 4 h on Stream at 400°C

Catalyst	Cumene cracking (oxides)				Cumene hydrocracking (reduced)				Cumene hydrocracking (sulfided)				Thiophene HDS
	% Conv.	% Yields			% Conv.	% Yields			% Conv.	% Yields			% Conv.
		Benz.[a]	αMS[b]	ΣSCC[c]		Benz.	αMS	ΣSCC		Benz.	αMS	ΣSCC	
A1	2.9	0.5	2.4	0	0.5	0	0.5	0	0	0	0	0	0
A2	34.5	0	31.0	3.5	5.1	1.8	1.6	1.7	5.0	1.5	2.0	1.4	24
A3	33.0	3.0	25.5	4.5	43.1	36.1	0.6	6.4	75.2	71.7	0	3.5	21
A4	39.9	2.9	29.4	7.5	76.4	70.0	0	6.6	78.7	76.1	0	2.4	19
A5	37.0	8.2	23.7	5.1	67.8	63.8	0.2	3.8	71.7	70.0	0.5	1.2	16
A6	71.4	68.8	2.6	0	82.3	82.3	0	0	80.6	80.2	0	0.4	0
A7	69.6	67.7	1.6	0.3	73.4	73.4	0	0	81.4	81.4	0	0	0
C1	19.3	0	18.9	0.4	1.3	0	1.3	0	1.6	0	1.6	0	0
C2	60.6	0	59.1	1.5	Not tested				Not tested				10
C3	63.5	0	62.7	0.8	Not tested				Not tested				8
C4	52.7	0	51.3	1.4	1.1	0	1.1	0	1.0	0	1.0	0	9
C5	57.5	0	56.0	1.5	Not tested				Not tested				10
C6	18.0	0	18.0	0	Not tested				Not tested				0
C7	19.4	0	19.4	0	1.6	0	1.6	0	Not tested				0
CA1	8.9	0	8.9	0	0.9	0	0.9	0	1.1	0	1.1	0	0
CA2	35.1	0	32.8	2.3	2.9	0.9	1.6	0.4	3.5	1.7	1.3	0.4	22
CA3	Not tested				12.6	9.5	1.3	1.8	14.7	11.2	1.1	2.3	17
CA4	42.1	5.6	32.2	4.3	34.0	30.4	1.0	2.6	42.9	37.6	0.7	4.6	16
CA5	42.4	12.8	26.9	2.7	60.9	57.8	0.5	2.6	58.3	52.1	0	6.2	11
CA6	58.4	52.9	5.5	0	35.2	34.3	1.0	0	49.0	48.3	0.7	0	0
CA7	64.7	60.6	4.1	0	49.5	48.7	0.8	0	49.7	48.8	0.8	0.1	0
AC2	20.4	0	20.4	0	1.6	0	1.6	0	2.2	0	1.7	0.4	6
AC3	20.2	0	20.2	0	2.3	0.8	1.5	0	5.9	2.8	1.5	1.6	4
AC4	12.4	0	12.3	0	4.3	3.2	1.1	0	7.9	4.9	1.7	1.3	4
AC5	36.7	10.9	22.8	3.0	22.7	21.4	1.2	0	27.4	25.3	1.1	1.0	3
AC6	16.8	10.0	6.8	0	2.7	1.7	1.0	0	4.3	3.1	1.2	0	0
AC7	38.5	32.1	6.4	0	10.2	9.4	0.7	0.1	11.2	10.2	0.8	0.2	0

[a] Benzene.
[b] α-Methylstyrene.
[c] Sum of side-chain cracking products (excluding benzene).

metal species and fluoride accumulate to some extent in the smaller pores of the catalysts and that the metal species effectively block these pores (hence a large decrease in surface area occurs) while the smaller fluoride ions do not. Such an accumulation of the active species may be expected to occur during the drying stage of the catalyst preparation where the larger pores empty of solution first and the receding liquid film carries solute into the smaller pores (21). Extending this argument to the AC series of catalysts, we may conclude that the large decrease in surface area resulting from the carbon coating of γ-alumina or F^-/Al_2O_3 arises from carbon deposition in smaller pores, while for the metal-containing catalysts only a small decrease in surface area is observed because these pores are already blocked by the metal species and the carbon deposition occurs in islands on the metals themselves.

To investigate this possibility, pore size distribution data for some of the catalysts was obtained by mercury porosimetry. The changes in pore volume for pores in the 8–12 nm diameter range were consistent with the changes in surface area measured by N_2 adsorption listed in Table 1. γ-alumina (A1) and F/Al_2O_3 (A6) had pore volumes of 0.32 and 0.30 cm^3g^{-1}, respectively, in this pore diameter range, while $C-Al_2O_3$ (CA1) and $C-F/Al_2O_3$ (AC6), which both have comparable wt% C, had pore volumes of 0.23 and 0.21 cm^3g^{-1}, respectively. In contrast, carbon coating of γ-alumina or F/Al_2O_3, and Ni–Mo impregnation do not affect the pore volume of the macropores (pores > 50 nm diameter). If a contact angle of 127° is taken for γ-alumina (22), and if it is assumed that $C-Al_2O_3$ presents a "carbon-like" surface to the mercury with an appropriate contact angle of 140° (23), then the average pore diameters are 7.0 and 8.4 nm, respectively. Such an upward shift in pore diameter, consistent with carbon deposition in the smaller pores of alumina, has also been observed by Vissers et al. (24) using N_2 adsorption–desorption isotherms (13.9 nm for γ-alumina

compared to 14.8 nm for a 35 wt% C on alumina catalyst). A similar shift in average pore diameter was also apparent for F/Al_2O_3 (A6) compared to $C-F/Al_2O_3$ (AC6). However, for the composite surfaces used in this study there is some uncertainty in the liquid–solid contact angle (25) and therefore caution should be employed when these types of comparisons are made.

It should be noted that Vissers et al. saw carbon deposition in the larger pores of γ-alumina for other carbon-coated alumina samples (14) during cyclohexene pyrolysis as opposed to the smaller pores, but they also observed an increase in surface area whereas we observed a decrease in surface area. An alternative explanation more in keeping with the findings of Vissers et al. is that carbon deposition on γ-alumina and F^-/Al_2O_3 catalysts occurs indiscriminately and uniformly as a thin layer over the support surface. In the presence of metals, however, carbon deposition occurs preferentially at the metal sites and generates multilayer islands of deposited carbon. This is supported by the observed decreases in surface areas between the A and AC catalyst series. When carbon deposition occurs as a thin monolayer on the alumina surface an associated large decrease in surface area is observed (40–50 m^2g^{-1}). In contrast, when deposition occurs only on certain sites on the surface far smaller decreases in surface area ensue (5–20 m^2g^{-1}). This fails to explain why the fluoride-associated Brønsted acid sites are so effectively poisoned by the "indiscriminate" carbon deposition, however.

Carbon coating of the alumina catalysts (AC series) may provide some insights into the mechanism of coking on this type of catalyst if it is assumed that the mechanisms of coking and pyrolysis are similar. There is some validity to this assumption since although neither mechanism is well understood they must both involve polymerization of olefins to some extent (12, 26). Interestingly, the active sites for pyrolysis of cyclohexene appear to be associated with the metal additives, rather than fluoride,

since the wt% C on AC6 and AC7 is similar to that on alumina alone (CA1) whereas the wt% C on the metal–containing catalysts is somewhat higher. Clearly, for a molecule such as cyclohexene which does not polymerize easily over acidic sites, fluoride promotion has little effect on the coking propensity. Fluoride promotion does increase the coking propensity for species which polymerize more easily, however, such as α-methylstyrene. This is discussed in the next section.

A notable feature of these results is that considerable carbon deposition occurs on the metal sites. It has been established that MoO_3 increases both the Brønsted and Lewis acidity on alumina (20, 27). The possibility that it is the Mo-associated Brønsted acid sites which are responsible for cyclohexene polymerization seems unlikely on the basis of the carbon deposition over the F-/Al_2O_3 catalysts. The polymerization may be associated with the increased Lewis acidity, however. Scaroni et al. (28) observed a reduction in coking of a Co–Mo/Al_2O_3 catalyst after it had been exposed to pyridine, a Lewis base. This led them to the conclusion that coking occurs to some extent on the Lewis acid sites on these types of catalysts. Alternatively, the metal centers themselves may be responsible for promotion of cyclohexene polymerization, suggesting that the increased coking propensity found for alumina-supported as compared to carbon-supported catalysts not only is related to the acidity of the alumina but also is somehow related to the metal–support interaction. At high loadings of fluoride (AC5) a higher weight percent carbon is deposited, suggesting that only at such fluoride concentrations is the acidity sufficient to polymerize cyclohexene on the fluoride-associated Brønsted acid sites.

Cumene Cracking

Cumene cracking involves the reaction of cumene over a catalyst in the absence of H_2. The formation of α-methylstyrene provides an indication of the dehydrogenation (and

therefore hydrogenation) ability of the catalyst, while benzene production is indicative of many/strong Brønsted acid sites on the surface. Benzene may be produced in two ways: First, via protonation of the aromatic ring on acidic sites, followed by cleavage of the ring–side-chain bond (29); second, via a mechanism involving dehydrogenation over the metal phase to form α-methylstyrene followed by protonation over the Brønsted acid sites and subsequent rearrangements and/or cleavage reactions (15). This second mechanism also gives rise to other side-chain-cracked products (SCC). The results of cumene cracking over the four series of catalysts are given in Table 2. Comparison of the activity of the three types of supports alone, carbon, alumina, and carbon-covered alumina, reveals the effect of carbon in this reaction. Carbon is the most active support of the three, producing 19% α-methylstyrene and so demonstrating the good hydrogenation–dehydrogenation properties of this support. Alumina, which has few hydrogenation–dehydrogenation sites, shows low activity in this reaction. Interestingly, the C-covered alumina support is more active in α-methylstyrene production than alumina, which implies that the deposited carbon is active in this reaction. This improved hydrogenation–dehydrogenation activity may be important from an industrial viewpoint where the promotion of hydrogen uptake is an essential property of a hydrotreating catalyst.

The effect of fluoride impregnation on the alumina support has been discussed previosly (20): Fluoride, by polarizing the alumina lattice, generates Brønsted acid sites which are very active in cracking cumene to benzene. We were gratified to see, as anticipated, that a similar promotion by fluoride of C–Al_2O_3 is possible and high production of benzene is also seen for the fluoride-containing CA catalysts. This indicates that some of the alumina lattice remains unchanged by the carbon deposition and that fluoride impregnation creates Brønsted acid sites on this part of the support. Carbon,

which has few surface hydroxyls is incapable of developing any Brønsted acidity upon addition of fluoride, hence no benzene is seen over the C series of catalysts. In fact, the presence of fluoride has no apparent effect on the carbon support; C6 and C7 both have comparable activity to C1.

The presence of the metals improves the hydrogenation–dehydrogenation ability of all the catalysts as reflected in the increased α-methylstyrene production. The carbon-supported catalysts are superior in this regard, followed by the CA then A series. In certain cases the improved dehydrogenation activity cannot be explained simply in terms of the greater activity of the carbon support. Possibly the metals have a higher dispersion, or the metals are more active on the inert carbon support. In either case, the slightly higher α-methylstyrene production over the CA catalysts, as compared to the A catalysts, may indicate that some of the metals are impregnated on the deposited carbon and that these sites are more active in this reaction than metal sites on the alumina part of the support.

The higher benzene yields over the CA catalysts compared to the alumina catalysts may be a direct result of the increased α-methylstyrene production since this may react further on the Brønsted acid sites to form benzene. Alternatively, the impregnated fluoride ions may be more concentrated on the exposed alumina surface thus producing stronger Brønsted acid sites.

With the exception of AC5 and AC7, carbon deposition onto the alumina catalysts appears to poison both the metal sites and the fluoride-associated Brønsted acid sites. As discussed earlier, pyrolysis of cyclohexene appears to occur preferentially on the metal sites of the catalysts, and so poisoning of both acid and dehydrogenation sites by carbon necessarily implies that these sites are in close proximity. It is interesting that only those catalysts with the highest fluoride loadings (AC5 and AC7) remain active in cumene cracking to benzene (see also the

hydrocracking results). Extending the argument in the previous Section we might conclude that at high F^- loadings a portion of the impregnated fluoride ions remains outside of the small pores where the carbon is deposited and thus some acidity remains. Another notable feature is that, in spite of the large amount of carbon deposited on the metal sites, substantial α-methylstyrene is still formed. Thiophene HDS studies indicate that these metal sites are indeed blocked, leading to the conclusion that it is the deposited carbon itself which is active in α-methylstyrene production.

Cumene Hydrocracking

Cumene hydrocracking involves the reaction of cumene over a catalyst in the presence of H_2. This reaction is a common probe for investigating the Brønsted acidity of catalysts since the presence of Brønsted acid sites results in cracking of the side-chain to form benzene or other side-chain cracked products. The results for cumene hydrocracking over the four series of catalysts, in their reduced and sulfided forms, are given in Table 2. Only a select few of the carbon-supported catalysts were tested in this reaction since the activity of all these catalysts is expected to be very low because of the lack of acidic hydroxyl functionalities on this support. The results of the few that were tested confirm the lack of Brønsted acidity on the carbon support.

The results on the A series of catalysts were similar to that observed previously (17), namely, that benzene is the major product for cumene hydrocracking over these catalysts and that the amount of benzene formed increases with increasing fluoride content. Also, the sulfided catalysts are more acidic than their reduced counterparts. Similar trends were observed on the CA catalysts although these surfaces were less acidic than the analogous A catalysts, probably a consequence of the smaller exposed alumina surface and therefore fewer Brønsted acid sites. The sulfided CA cata-

lysts were not found to be especially more active than the reduced counterparts unlike the A series analogs.

The results of the AC catalysts again indicate poisoning of the active sites by the deposited carbon. For the catalysts containing the highest fluoride loading some Brønsted acid sites persist, as evidenced by higher benzene yields for AC5 and AC7. The acidity of these two catalysts is lower than anticipated on the basis of their cumene cracking results (note that for the A catalysts much more benzene is produced under hydrocracking than under cracking conditions). This tends to suggest that much of the benzene produced over these catalysts under cracking conditions is via mechanism 2 (dehydrogenation followed by protonation and then cleavage) and under hydrocracking conditions this mechanism is suppressed by H_2. This provides additional evidence that, at least for AC7 which contains no metals, dehydrogenation occurs over the deposited carbon.

Thiophene HDS

Up until this point in our investigations the results for the new support system, F^-/ $C–Al_2O_3$, were very promising. The cumene reaction studies indicated that acidity could easily be developed on the alumina part of the support and that, in spite of its low surface area, the deposited carbon participates in dehydrogenation (and presumably hydrogenation) reactions. The results in Table 2 indicate that those catalysts containing fluoride only had little or no activity in thiophene HDS, indicating (not unexpectedly) that the metals form the active sites in this reaction. The most perplexing and disappointing feature of our results is the exceptionally low activity of the carbon-supported catalysts in this reaction. This was unexpected since it has been reported that carbon is a superior support to alumina in thiophene HDS (24, 30–31). Changing the catalyst preparation method, sulfiding temperature, reaction temperature, and re-

actant flow rates did not alter the result that carbon was a poorer support for thiophene HDS than alumina. However, it should be noted that only one metal loading was studied and there is a suggestion in the literature that the comparative activities of carbon versus γ-alumina may be metal-concentration-dependent (30). In view of the results for the carbon-supported catalysts it is perhaps not surprising to find that our CA catalysts did not have the improved HDS activity reported by Vissers et al. which had prompted us to pursue this work. The CA catalysts did have comparable activity to the alumina catalysts, however.

Deactivation Studies

Of the model reactions studied only the cumene cracking deactivation curves were found to be very informative. Figure 3 shows the percent conversions in cumene cracking for the four series of catalysts as a function of time. On the alumina support, catalysts containing fluoride additive only have nearly constant activity with time (over the interval studied) and the product distribution is nearly 100% benzene. The AC and CA catalysts behave similarly to the alumina series although some deactivation of AC7 and CA7 is apparent over the 4 h reaction time. This deactivation is associated with a slight decrease in benzene production. In the presence of metals, however, marked deactivation does occur; a drop in activity of between 20–40% is observed for the alumina catalysts over 4 h, and a generally slower decrease in activity of about 25% of the initial activity over 4 h for the carbon-coated alumina catalysts. The product distribution contains both α-methylstyrene and benzene and other side-chain cracked products. An example of how the product distribution varies with time is given in Fig. 4 and it is clear from this that the drop in activity is associated with a rapid decrease in benzene formation, i.e., a rapid poisoning of acidic hydroxyls. Conversely, on the carbon-supported catalysts the cata-
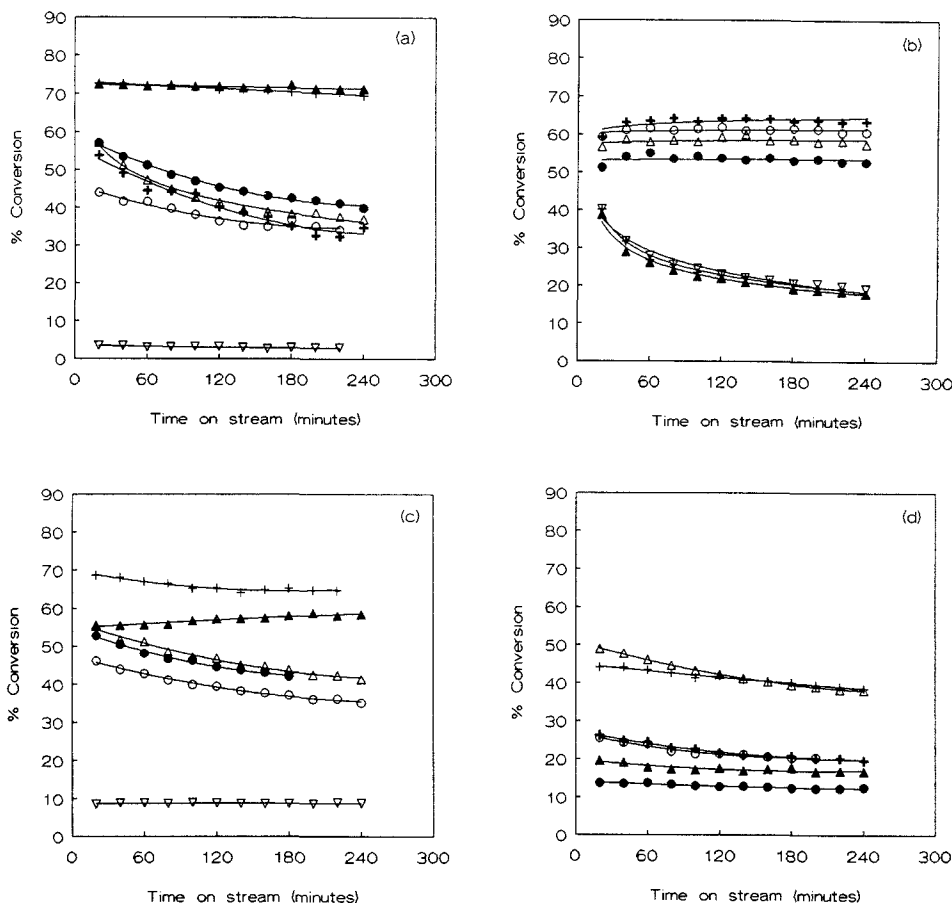
FIG. 3. Cumene cracking deactivation curves for Ni–Mo–F catalysts supported on (a) γ-alumina (A series), (b) carbon (C series) (c) carbon-covered alumina (CA series) and (d) carbon covered A series of catalysts (AC). NiO–MoO₃–F weight percents are ▽ 0-0-0, ○ 3-15-0, + 3-15-1.8, ● 3-15-3.6, △ 3-15-6.9, ▲ 0-0-3.6, and + 0-0-6.9, respectively.

lysts containing only fluoride deactivate rapidly with time (50% drop in activity over 4 h) while on the catalysts containing both metals and fluoride the activity stays almost constant with time. The only product in this case is α-methylstyrene.

The following conclusions may be drawn from these results: Since A, CA, and AC catalysts containing only fluoride do not deactivate rapidly, cracking to benzene over fluoride-associated Brønsted acid sites via protonation and then side-chain cracking does not coke the catalyst; i.e., propene produced by this mechanism behaves similarly

to cyclohexene in that it does not polymerize on the acid sites. The second mechanism for benzene formation, which involves dehydrogenzation over the metal sites followed by protonation over the fluoride-associated Brønsted acid sites and then cleavage and/or rearrangement, does poison acid sites through coking, however. This is evidenced for catalysts containing both F⁻ and Ni–Mo in a rapid decrease in the formation of cracked products as a function of time but only a slow decrease in α-methylstyrene production (Fig. 4), suggesting that it is the acid sites rather than the metal sites where
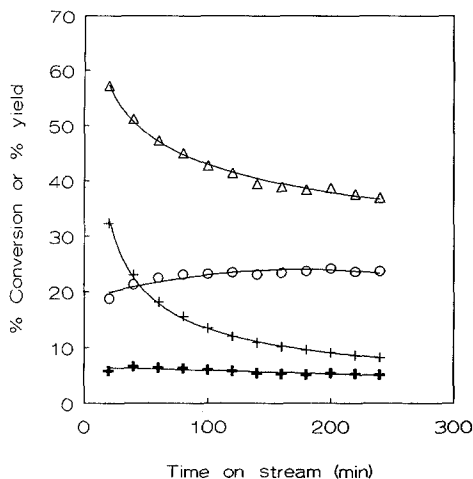
FIG. 4. Product distribution with time for catalyst A5 during cumene cracking. $\triangle$ % conversion, + % yield benzene, $\bigcirc$ % yield α-methylstyrene and + % yield others.

coking occurs; i.e., α-methylstyrene, which can polymerize easily, does so on the acid sites, thus coking them. The small deactivation of AC7 and CA7 suggests that some of the benzene produced over these catalysts is produced by the second mechanism, where dehydrogenation occurs over the deposited carbon rather than metal sites. On the carbon catalysts, which do not contain any Brønsted acid sites, this mechanism for benzene formation cannot take place, and therefore the activity remains constant with time.

CONCLUSIONS

Carbon-covered alumina may be prepared by pyrolysis of cyclohexene on either γ-alumina or boehmite, with boehmite presenting the slightly more active surface of the two. For both precursor supports a linear decrease in surface area with increasing weight percent carbon is observed, possibly a result of some low surface area carbon deposition in the smaller pores of the substrate. The carbon deposition follows adsorption isotherm-type behavior, with an apparent monolayer coverage of 26–31 wt%

C depending on the alumina precursor. At this carbon coverage some of the alumina surface is still accessible to small species such as fluoride ions but not to the larger cyclohexene or cumene molecules.

The carbon-covered alumina support merges the properties of carbon and alumina in that the deposited carbon is active in dehydrogenation while the exposed alumina surface may develop considerable Brønsted acidity through fluoride impregnation. In the thiophene HDS reaction the increased dehydrogenation activity did not translate into improved hydrogenation activity, however. It should be noted that this thiophene HDS reaction was performed under an approximately atmospheric pressure of hydrogen, whereas high H_2 pressures may be required before an improved hydrogenation activity is manifested. It is our intention, therefore, to extend this study to investigate these catalysts in the hydrotreating of a gas oil feed at high H_2 pressures to explore this possibility.

When cyclohexene is pyrolyzed on fluorided Ni–Mo/Al$_2$O$_3$ catalysts it is clear that the metal centers promote the polymerization, possibly through increasing the Lewis acidity of the support, but that the Brønsted acid sites generated by fluoride are not strong enough to effect this reaction. These Brønsted acid sites do promote polymerization (coke formation) of molecules which polymerize more easily, however, such as α-methylstyrene, which forms a more stable tertiary carbocation. Model compound reaction studies before and after carbon deposition show that both metal sites and fluoride-associated Brønsted acid sites are blocked by carbon. Catalyst characterization leads to the suggestion that catalytic species accumulate in smaller pores in the support during the preparation procedure and that carbon deposition also occurs preferentially at these locations.

The alumina-supported catalysts studied here were superior in the HDS reaction to analogous carbon catalysts. Previous studies have indicated that if the metal loading

per square nm of surface is identical, carbon is superior to alumina as a support (27). However, since the surface area of carbon is up to five times as large, such catalysts have a much higher metals loading than alumina, on a weight percent basis. The results obtained here suggest that if the metal loadings are comparable on a weight percentage basis, then alumina is a superior support for Ni–Mo catalysts.

REFERENCES

1. Vissers, J. P. R., Ph.D. Thesis, p. 7. Eindhoven University, The Netherlands, 1985.
2. Arnoldy, P., van den Heykant, J. A. M., deBok, G. D., and Moulijn, J. A., *J. Catal.* **92,** 35 (1985).
3. Burggraf, L. W., Leyden, D. E., Chin, R. L., and Hercules, D. M., *J. Catal.* **78,** 360 (1982).
4. Gates, B. C., Katzer, J. R., and Schuit, G. C. A., *in* "Chemistry of Catalytic Processes," p. 413. McGraw–Hill, New York, 1979.
5. deBeer, V. H. J., Derbyshire, F. J., Groot, C. K., Prins, R., Scaroni, A. W., and Solar, J. M., *Fuel* **63,** 1095 (1984).
6. Zdrazil, M., *J. Catal.* **58,** 436 (1979).
7. Topsøe, H., and Clausen, B. S., *Appl. Catal.* **25,** 273 (1986).
8. Ledoux, M. J., Michaux, O., Agostini, G., and Panissod, P., *J. Catal.* **102,** 275 (1986).
9. van Veen, J. A., Gerkema, E., van der Kraan, A. M., and Knoester, A., *Chem. Comm.,* 1684 (1987).
10. Vissers, J. P. R., deBeer, V. H. J., and Prins, R., *J. Chem. Soc. Faraday Trans. 1* **83,** 2145 (1987).
11. Abotsi, G. M. K., and Scaroni, A. W., *Fuel Process. Technol.* **22,** 107 (1989).
12. Youtsey, K. J., Holt, W. C., Carnahan, R. D., and Spielberg, D. H., U.S. Patent 4,018,943 (1977).
13. Butterworth, S. L., and Scaroni, A. W., *Appl. Catal.* **16,** 375 (1985).
14. Vissers, J. P. R., Mercx, F. P. M., Bouwens, S. M. A. M., de Beer, V. H. J., and Prins, R., *J. Catal.* **114,** 291 (1988).
15. Boorman, P. M., Kydd, R. A., Sarbak, Z., and Somogyvari, A., *J. Catal.* **100,** 287 (1986).
16. Boorman, P. M., Kydd, R. A., Sarbak, Z., and Somogyvari, A., *J. Catal.* **106,** 544 (1987).
17. Lewis, J. M., Kydd, R. A., and Boorman, P. M., *J. Catal.* **120,** 413 (1989).
18. Swift, E. H., and Schaefer, W. P., "Qualitative Elemental Analysis," p. 193. Freeman, San Francisco, 1962.
19. Chong, K., unpublished data.
20. Boorman, P. M., Kydd, R. A., Sarbak, Z., and Somogyvari, A., *J. Catal.* **96,** 115 (1985).
21. Le Page, J. F., *in* "Applied Heterogeneous Catalysis," p. 109. Éditions Technip, Paris, 1987.
22. ASTM Designation: D 4284-83, "Standard Test Method for Determining Pore Volume Distribution of Catalysts by Mercury Intrustion Porosimetry."
23. de Vooys, F., *in* "Activated Carbon . . . A Fascinating Material" (A. Capelle and F. de Vooys, Eds.,), p. 35. Norit N. V., The Netherlands, 1983.
24. Vissers, J. P. R., Lensig, T. J., Mercx, F. P. M., de Beer, V. H. J., and Prins, R., *presented at the* "Third International Seminar on Hydrogen as an Energy Carrier, Lyon, 1983."
25. Johnson, M. F. L., *J. Catal.* **110,** 419 (1988).
26. Pines, H., *in* "The Chemistry of Catalytic Hydrocarbon Conversions," p. 87. Academic Press, New York, 1981.
27. Segawa, K., and Hall, W. K., *J. Catal.* **76,** 113 (1982).
28. Scaroni, A. W., Jenkins, R. G., Utrilla, J. R., and Walker, P. L., Jr., *Fuel Process. Technol.* **9,** 103 (1984).
29. Pines, H., *in* "The Chemistry of Catalytic Hydrocarbon Conversions," p. 113. Academic Press, New York, 1981.
30. Duchet, J. C., van Oers, E. M., de Beer, V. H. J., and Prins, R., *J. Catal.* **80,** 386 (1983).
31. Vissers, J. P. R., Scheffer, B., de Beer, V. H. J., Moulijn, J. A., and Prins, R., *J. Catal.* **105,** 277 (1987).